

NOVEL DEVELOPMENTS AND FINDINGS FOR THE SAFETY ASSESSMENT OF EARTHQUAKE-EXCITED DAM-RESERVOIR SYSTEMS

N. Bouaanani¹, F. Lu², C. Perrault³, M.A. Chagnon², and I. Gogoi⁴

¹Associate Professor (email: najib.bouaanani@polymtl.ca), ²Research Graduate Assistant, ³Research Assistant
Department. of Civil, Geological and Mining Engineering, École Polytechnique de Montréal, Canada
⁴Lecturer, Department of Civil Engineering, Assam Engineering Institute, Guwahati, India

ABSTRACT :

Many dams worldwide have been in service over 50 years and are located in high seismicity areas. The initial seismic design of these critical structures was generally conducted using simplified methods that do not fully take into account of the dynamic nature of earthquake excitation and the complex fluid-structure interaction. Although significant work has been done to evaluate the seismic response of dams, there is still a need to improve commonly used simplified methods and to accurately assess the efficiency of more sophisticated ones. The first part of this paper proposes new practical formulas to evaluate earthquake-induced hydrodynamic loading on concrete dams. This original technique generalizes the classical added-mass formulation by including the effects of dam flexibility and reservoir bottom absorption. Frequency response functions of hydrodynamic pressures within the reservoir are compared to analytical solutions. It is shown that the method accurately predicts hydrodynamic loads and that it can be easily implemented in a computer program or a spreadsheet. The second part of the paper investigates finite element modeling aspects to assess the seismic performance of concrete dams. Several finite element models of dam-reservoir systems with various dimensions are used to conduct frequency and time domain analyses. Potential-based fluid elements and viscous boundary conditions are validated against analytical solutions and they are shown to perform adequately for practical seismic analysis of dam-reservoir systems.

KEYWORDS: Dam safety, Hydrodynamic loading, Seismic effects, Numerical modeling.

1. INTRODUCTION

Dam failures may result in catastrophic consequences, causing considerable loss of life and property. Research dealing with dam safety has been extensively active during the last 50 years to improve understanding of the complex behavior of dam-reservoir systems and implement more reliable approaches into the codes of practice. Rigorous techniques to investigate dynamic dam-reservoir interactions are relatively new compared to more established static dam analysis tools. The milestone of such rigorous treatment dates back to the pioneering work of Westergaard (1933), who proposed to model water action on a dam subjected to horizontal ground accelerations as an equivalent added mass height-wise distribution applied on the dam face. Although Westergaard's analytical solution neglected dam flexibility and water compressibility, it has been widely used for many decades to design earthquake resistant concrete dams. Dynamic interactions in dam-reservoir systems are complex phenomena requiring advanced mathematical and numerical modeling. Although available sophisticated techniques can handle many aspects of these phenomena, simplified procedures are useful and still needed to globally evaluate the effects of dam-reservoir interaction. This section of the paper proposes an original and practical procedure to evaluate earthquake induced dam-reservoir interactions, including the effects of dam flexibility, water compressibility and reservoir bottom wave absorption. In a previous work, the first author of the present paper proposed a simplified closed-form formulation to evaluate earthquake-induced hydrodynamic pressures on concrete dams (Bouaanani et al. 2003). The method includes the effects of water compressibility and reservoir bottom wave absorption. The influence of dam deformability was however neglected and therefore the total hydrodynamic pressure exerted on a dam during an earthquake could not be determined. The first part of this paper proposes a newly improved and practical formulation where the rigid dam restricting assumption is waived.

On the other hand, extensive work has been dedicated to the development of solid and fluid finite element formulations, and their implementation in fluid-structure interaction problems. Among these techniques, Eulerian-based formulations present several advantages and were successfully applied to transient wave propagation problems (Neilson et al. 1981; Everstine et al. 1983, Olson and Bathe 1985). In the second part of this paper, a potential-based formulation is adapted to investigate dam-reservoir systems. The formulation is validated against analytical solutions obtained over a wide frequency range.

2. SIMPLIFIED FORMULATION

2.1. Theoretical background

The simplified geometry of a dam-reservoir system is shown in Figure 1. The dam has a total height H_s and it impounds a semi-infinite reservoir of constant depth H_r . Sediments that may be deposited at reservoir bottom are also considered. A Cartesian coordinate system with axes x and y with origin at the heel of the structure is adopted and the following main assumptions are made: (i) the dam and the water are assumed to have a linear behavior; (ii) the water in the reservoir is compressible and inviscid, with its motion irrotational and limited to small amplitudes; and (iii) gravity surface waves are neglected. Under these assumptions, the hydrodynamic pressure $p(x,y,t)$ in the reservoir (in excess of the hydrostatic pressure) obeys the wave equation

$$\nabla^2 p = \frac{1}{C_r^2} \frac{\partial^2 p}{\partial t^2} \quad (2.1.1)$$

where ∇^2 is the Laplace differential operator, t the time variable; ρ_r the mass density of water and C_r the compression wave velocity given by

$$C_r = \sqrt{\frac{\mu_r}{\rho_r}} \quad (2.1.2)$$

in which μ_r denotes the bulk modulus of water.

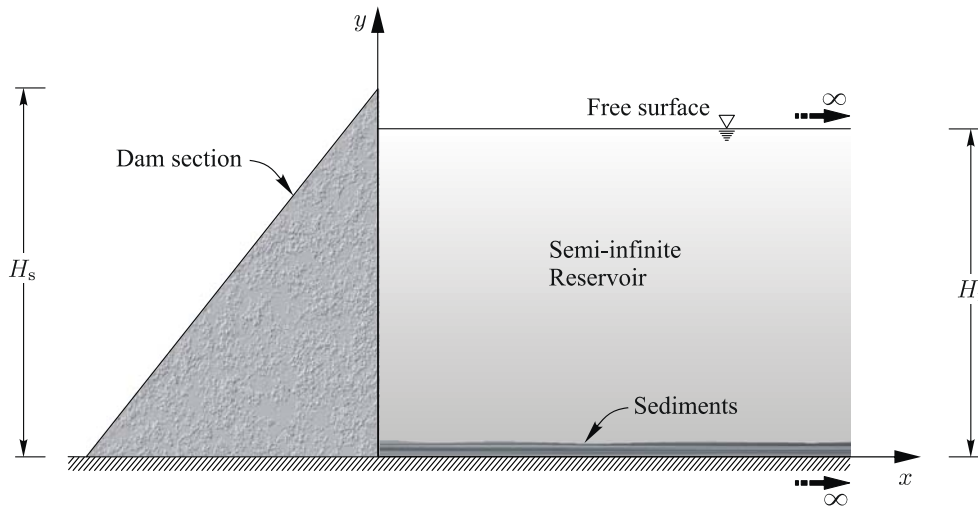


Figure 1. Dam-reservoir system with a simplified geometry.

Considering harmonic ground motions, hydrodynamic pressure in the reservoir can then be expressed in frequency domain as $p^{(\xi)}(x,y,t) = \bar{p}^{(\xi)}(x,y,\omega) e^{i\omega t}$ where the superscript (ξ) denotes the x or y earthquake direction, ω the exciting frequency, and $\bar{p}^{(\xi)}(x,y,\omega)$ a complex-valued frequency response function. Introducing this transformation into Eqn. 2.1.1 yields the classical Helmholtz equation

$$\nabla^2 \bar{p}^{(\xi)} + \frac{\omega^2}{C_r^2} \bar{p}^{(\xi)} = 0; \quad \xi = x, y \quad (2.1.3)$$

The complex valued pressure frequency response functions $\bar{p}^{(\xi)}$ along directions $\xi = x, y$ can be expressed as (Fenves and Chopra 1984)

$$\bar{p}^{(\xi)}(x, y, \omega) = \bar{p}_0^{(\xi)}(x, y, \omega) - \omega^2 \sum_{j=1}^{m_s} \bar{Z}_j^{(\xi)}(\omega) \bar{p}_j(x, y, \omega); \quad \xi = x, y \quad (2.1.4)$$

where $\bar{p}_0^{(\xi)}$ is the frequency response function for the hydrodynamic pressure at rigid dam face due to ground acceleration along $\xi = x, y$ direction, \bar{p}_j is the frequency response for hydrodynamic pressure due to horizontal acceleration $\psi_j^{(x)}(y) = \psi_j^{(x)}(0, y)$ of the dam upstream face, $\bar{Z}_j^{(\xi)}$ is the generalized coordinate along earthquake excitation direction ξ , and m_s the total number of mode shapes included in the analysis. Throughout this paper, hydrodynamic pressures $\bar{p}_0^{(\xi)}$ and \bar{p}_j will be referred to as the “rigid” and the “flexible” parts of the total hydrodynamic pressure \bar{p} , respectively. The boundary conditions to be satisfied by hydrodynamic frequency response functions translate compatibility of pressures and displacements at dam-reservoir interface and wave absorption at reservoir bottom (Fenves and Chopra 1984). Boundary conditions to model free surface, gravity waves or the presence of an ice cover at reservoir surface were also proposed (Bouaanani et al. 2003). The complex frequency response functions of hydrodynamic pressures $\bar{p}_0^{(x)}$ and \bar{p}_j can then be expressed as the summation of m_r response functions $\bar{p}_{0n}^{(\xi)}$ and \bar{p}_{jn} corresponding each to a reservoir mode n

$$\bar{p}_0^{(x)}(x, y, \omega) = \sum_{n=1}^{m_r} \bar{p}_{0n}^{(x)}(x, y, \omega) = -2\rho_r a_g^{(x)} H_r \sum_{n=1}^{m_r} \frac{\lambda_n^2(\omega)}{\beta_n(\omega)} \frac{I_{0n}(\omega)}{\kappa_n(\omega)} e^{\kappa_n(\omega)x} Y_n(y, \omega) \quad (2.1.5)$$

$$\bar{p}_j(x, y, \omega) = \sum_{n=1}^{m_r} \bar{p}_{jn}(x, y, \omega) = -2\rho_r H_r \sum_{n=1}^{m_r} \frac{\lambda_n^2(\omega)}{\beta_n(\omega)} \frac{I_{jn}(\omega)}{\kappa_n(\omega)} e^{\kappa_n(\omega)x} Y_n(y, \omega) \quad (2.1.6)$$

where λ_n and Y_n are complex-valued frequency dependent eigenvalues and orthogonal eigenfunctions satisfying, for each reservoir mode n

$$e^{2i\lambda_n(\omega)H_r} = -\frac{\lambda_n(\omega) - \omega q}{\lambda_n(\omega) + \omega q} \quad (2.1.7)$$

$$Y_n(y, \omega) = \frac{[\lambda_n(\omega) - \omega q] e^{-i\lambda_n(\omega)y} + [\lambda_n(\omega) + \omega q] e^{i\lambda_n(\omega)y}}{2\lambda_n(\omega)} \quad (2.1.8)$$

and where the terms $\beta_n, \kappa_n, I_{0n}$ and I_{jn} are given by

$$\beta_n(\omega) = H_r [\lambda_n^2(\omega) - \omega^2 q^2] + i\omega q; \quad \kappa_n(\omega) = \sqrt{\lambda_n^2(\omega) - \frac{\omega^2}{C_r^2}} \quad (2.1.9)$$

$$I_{0n}(\omega) = \frac{1}{H_r} \int_0^{H_r} Y_n(y, \omega) dy; \quad I_{jn}(\omega) = \frac{1}{H_r} \int_0^{H_r} \psi_j^{(x)}(y) Y_n(y, \omega) dy \quad (2.1.10)$$

2.2. Simplified expressions

The x -component of the structural mode shape ψ_j can be approximated as a polynomial function

$$\psi_j^{(x)}(y) = \sum_k a_k \left(\frac{y}{H_s} \right)^k \quad (2.2.1)$$

where y is the coordinate varying over the height of the structure measured from the bottom. We show then that

the rigid and flexible hydrodynamic pressures at acoustical mode n are related by

$$\bar{p}_{jn}(x, y, \omega) = \frac{\bar{p}_{0n}^{(x)}(x, y, \omega)}{a_g^{(x)}} \left[F_{jn}(\omega) + \frac{G_{jn}(\omega)}{I_{0n}(\omega)} \right] \quad (2.2.2)$$

in which

$$F_{jn}(\omega) = \sum_k \left\{ \left[\sum_{l=0}^k (-1)^{k-l} \frac{\Lambda_{2l}(\lambda_n H_r)}{\Lambda_{2k}(\lambda_n H_s)} \right] a_{2k} + \left[\sum_{l=0}^k (-1)^{k-l} \frac{\Lambda_{2l+1}(\lambda_n H_r)}{\Lambda_{2k+1}(\lambda_n H_s)} \right] a_{2k+1} \right\} \quad (2.2.3)$$

$$G_{jn}(\omega) = -\frac{i\omega q}{\lambda_n^2 H_r} F_{jn}(\omega) + \frac{1}{\lambda_n H_r} \sum_k \left\{ \left[\frac{i\omega q}{\lambda_n} \frac{(-1)^k}{\Lambda_{2k}(\lambda_n H_s)} \right] a_{2k} - \left[\frac{(-1)^k}{\Lambda_{2k+1}(\lambda_n H_s)} \right] a_{2k+1} \right\} \quad (2.2.4)$$

and where the complex-valued function A_m is defined by

$$A_m(z) = \frac{z^m}{m!} \quad (2.2.5)$$

for complex and integer numbers, z and m , respectively. This important and original relation relates the flexible and rigid parts of hydrodynamic pressure for a given reservoir acoustical mode to the vibration of the structure along a given mode shape. The rigid pressure can then be determined using closed-form expressions similar to those developed by the first author of this paper (Bouaanani et al. 2003). These expressions take account of water compressibility and wave absorption at reservoir bottom and they were shown valid for a wide frequency range.

2.3. Numerical application

The simplified method presented in the previous section is applied to a simplified triangular dam cross-section with geometry inspired from the tallest non-overflow monolith of Pine Flat dam (Fenves and Chopra 1984). The dam has a height $H_s = 121.92$ m, a downstream slope of 0.8 and a vertical upstream dam face. The following dam material properties are selected: a Poisson's ratio $\nu_s = 0.2$ and a mass density $\rho_s = 2400$ kg/m³. Two values of modulus of elasticity $E_s = 25000$ MPa and $E_s = 35000$ MPa are considered. The water is assumed compressible, with a velocity of pressure waves $C_r = 1440$ m/s, a mass density $\rho_r = 1000$ kg/m³ and a bulk modulus $\nu_r = 2.1 \times 10^3$ MPa. A cubic profile is chosen to approximate the first structural mode shape $\psi_1^{(x)}$. Eqns. 2.2.3, 2.2.4 and 2.2.2 are used to determine the response functions F_{jn} , G_{jn} and \bar{p}_{1n} . Eqn. 2.1.4 is then used to compute the hydrodynamic pressure frequency response functions illustrated in Figure 2. Frequency responses are plotted against the frequency ratio ω/ω_1 where ω_1 is the fundamental vibration frequency of the dam on rigid foundation with an empty reservoir. A sufficient number of reservoir modes $N_r=5$ is included in the analysis. The figure shows an excellent agreement between the simplified formulation and the analytical solution. We also observe that the quality of the approximation does not decay as wave reflection coefficient decreases.

3. FINITE ELEMENT MODELING

3.1. Potential-based formulation

The analytical formulation presented above includes the combined effects of water compressibility, dam flexibility and wave absorption at reservoir bottom. It is however restrained by the simplified rectangular geometry of the impounded reservoir. In this section a $\phi-U$ potential-based formulation is used to investigate dam-reservoir-foundation systems with irregular geometries. Assuming an irrotational water motion and infinitesimal velocity and density changes, implies the existence of a velocity potential $\phi(x, y, t)$ satisfying the equations of continuity and energy conservation (Landau and Lifshitz 1959)

$$\nabla^2 \phi = \frac{1}{C_r^2} \frac{\partial^2 \phi}{\partial t^2} \quad (3.1.1)$$

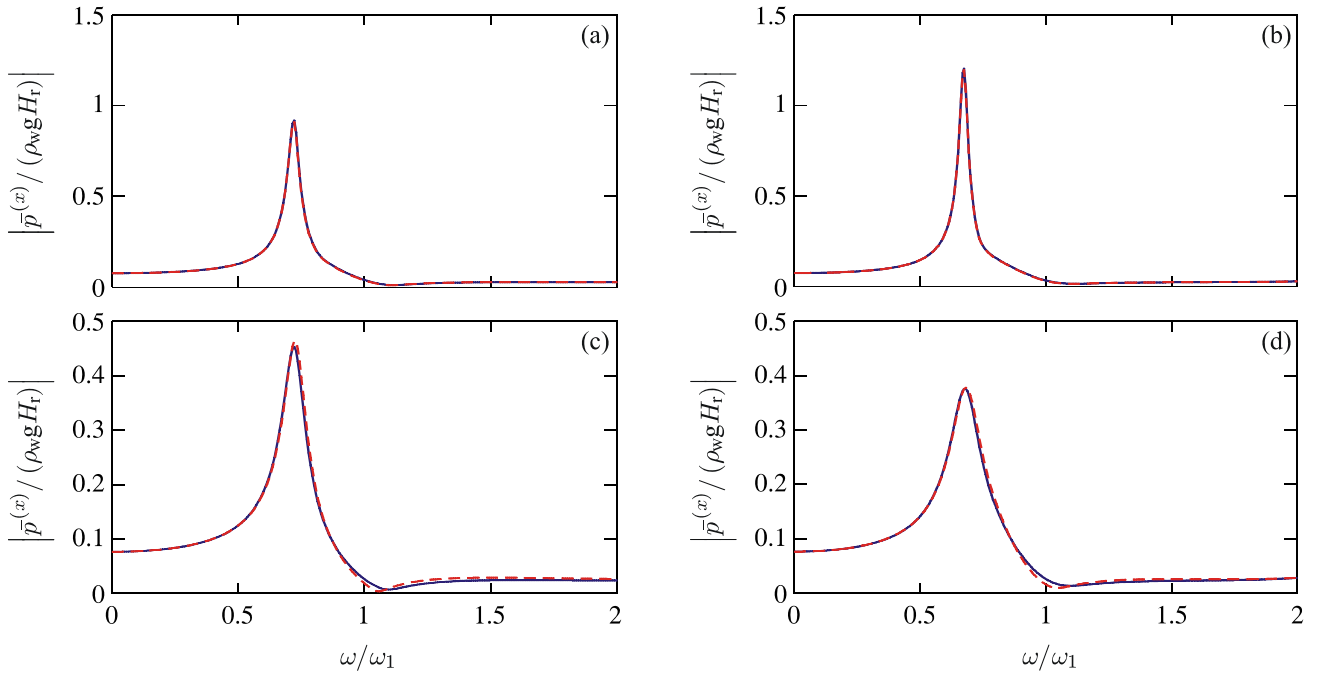


Figure 2. Absolute value of frequency response functions of normalized hydrodynamic pressure at dam heel: (a) $\alpha = 0.95$ and $E_s = 25000$ MPa; (b) $\alpha = 0.95$ and $E_s = 35000$ MPa; (c) $\alpha = 0.65$ and $E_s = 25000$ MPa; (d) $\alpha = 0.65$ and $E_s = 35000$ MPa; – Analytical solution; -- Simplified formulation.

Eqn. 3.1.1 is associated to the essential boundary condition

$$\phi = 0 \quad (3.1.2)$$

on the free surface and rigid boundaries, and to the natural boundary condition

$$\frac{\partial \phi}{\partial n} = \dot{u}_n \quad (3.1.3)$$

on moving fluid-structure interfaces with positive normal velocity \dot{u}_n , corresponding to unit surface normal vector \mathbf{n} pointing into the fluid and out of the structure.

Using standard techniques, the weak variational form of Eqn. 3.1.1 can be obtained

$$\frac{\rho_r}{C_r^2} \int_{V_r} \ddot{\phi} \delta \phi dV + \rho_r \int_{S_r} \dot{u}_n \delta \phi dS + \rho_r \int_{V_r} \nabla \phi \cdot \nabla \delta \phi dV = 0 \quad (3.1.4)$$

in which V_r indicates the reservoir domain, and S_r a reservoir boundary where normal velocity is prescribed. Under earthquake excitation, the dynamic response of the dam and the reservoir are coupled through compatibility of velocity potential (*resp.* hydrodynamic pressure) and prescribed normal velocity (*resp.* normal acceleration) at dam-reservoir interface. Dam-reservoir interaction is contained in the second term of Eqn. 3.1.4. Figure 3 shows a finite element mesh of a dam monolith impounding a reservoir with an irregular shape. Using classical Galerkin discretization, the coupling between the dam and reservoir sub-structures yields the system of equations

$$\begin{bmatrix} \mathbf{M}_{ss} & \mathbf{0} \\ \mathbf{0} & -\mathbf{M}_{rr} \end{bmatrix} \begin{bmatrix} \ddot{\mathbf{U}} \\ \ddot{\Phi} \end{bmatrix} + \begin{bmatrix} \mathbf{C}_{ss} & \mathbf{C}_{sr} \\ \mathbf{C}_{rs} & \mathbf{C}_{rr} \end{bmatrix} \begin{bmatrix} \dot{\mathbf{U}} \\ \dot{\Phi} \end{bmatrix} + \begin{bmatrix} \mathbf{K}_{ss} & \mathbf{0} \\ \mathbf{0} & -\mathbf{K}_{rr} \end{bmatrix} \begin{bmatrix} \mathbf{U} \\ \Phi \end{bmatrix} = \begin{bmatrix} -\mathbf{M}_{ss} \mathbf{1}^{(\xi)} \ddot{u}_g^{(\xi)}(t) \\ -\mathbf{C}_{rs} \mathbf{1}^{(\xi)} \dot{u}_g^{(\xi)}(t) \end{bmatrix} \quad (3.1.5)$$

where vectors \mathbf{U} and Φ contain the nodal displacements relative to the ground and the nodal velocity potentials, respectively.

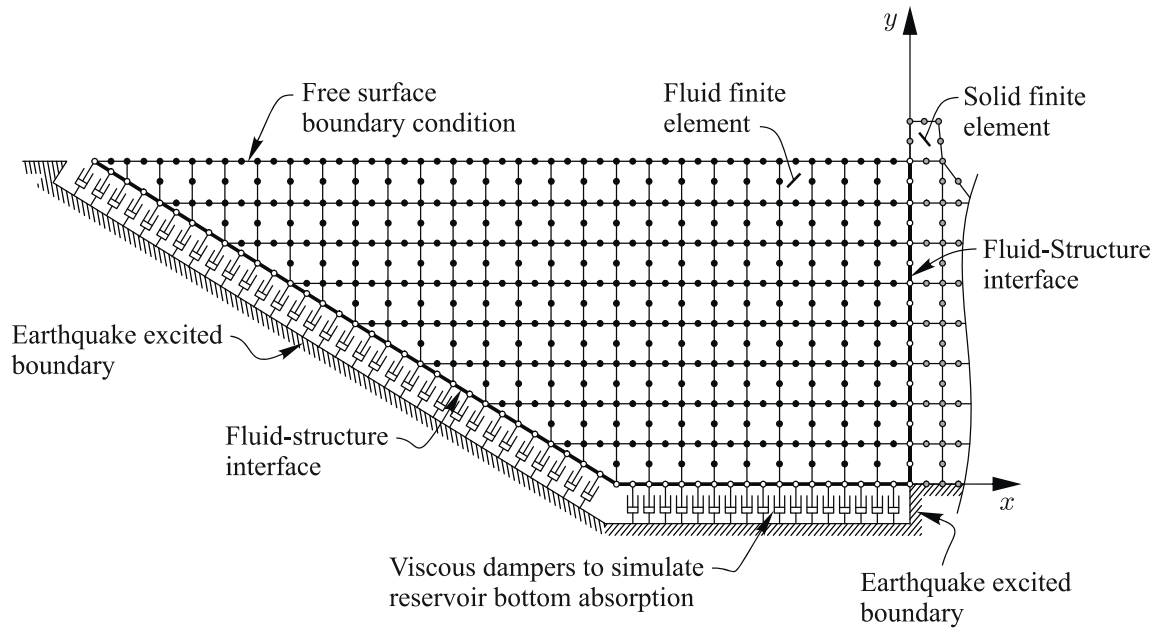


Figure 3. Finite element model a dam-reservoir system and corresponding boundary conditions.

Sub-matrices \mathbf{M}_{ss} and \mathbf{K}_{ss} represent the mass and stiffness matrices for the dam substructure, and \mathbf{M}_{rr} and \mathbf{K}_{rr} those for the reservoir. A Rayleigh damping matrix \mathbf{C}_{ss} is considered for the dam substructure and sub-matrices \mathbf{C}_{rs} and \mathbf{C}_{sr} account for dam-reservoir interaction through enforced equilibrium and compatibility at fluid-structure interface as illustrated in Figure 3. Sub-matrix \mathbf{C}_{rr} accounts for damping due to energy dissipation at the bottom and/or at the far upstream boundary of the reservoir and is given by

$$\mathbf{C}_{rr} = \rho_r q \int_{S_r} \mathbf{N}_r^T \mathbf{N}_r dS \quad (3.1.6)$$

in which N_r is a standard isoparametric shape function matrix for fluid elements and S_s denotes surface of the reservoir bottom boundary. Using the technique proposed by Lysmer and Kuhlemeyer (1969), the absorptive condition at reservoir bottom can be approximated by a series of viscous dampers placed at the reservoir-foundation interface. To ensure compatibility between fluid and damper elements and enable fluid-structure interaction, isoparametric beam elements are inserted along reservoir-foundation interface. Damper elements are then built by connecting beam element nodes to the ground. Damper and beam element nodes are constrained to move only perpendicularly to the reservoir bottom boundary. In the next section, the potential-based formulation and boundary conditions described previously are confronted against analytical solutions when available or boundary element solutions otherwise.

3.2. Numerical results

Gravity dam monoliths impounding reservoirs with different shapes were analysed using the potential-based formulation presented above. Results are shown for the same triangular dam cross-section described in section 2.3. The finite element models are built using the software ADINA (2006). The dam and reservoir are modeled using 9-node isoparametric plane stress finite elements including incompatible modes and 9-node potential-based finite elements, respectively. Analytical and finite element solutions are presented in Figure 4 for a rectangular reservoir length $L_r = 2H_s$ and height $H_r = H_s$. We consider frequency sweep ratios ω/ω_0 varying from 0 to 4 where $\omega_0 = \pi C_r/(2H_r)$ denotes the natural frequency of the full reservoir. The figure illustrates an excellent agreement between the results of potential-based fluid elements and the analytical solution is excellent for the rigid case. It is seen that dam flexibility and structural damping affects the accuracy of the results with some slight discrepancies appearing at higher frequencies larger than $3\omega_0$. Figure 5 illustrates the effects of reservoir shape and wave absorption at reservoir bottom. The viscous boundary condition described in the previous section is applied along the reservoir bottom using consistent lumping.

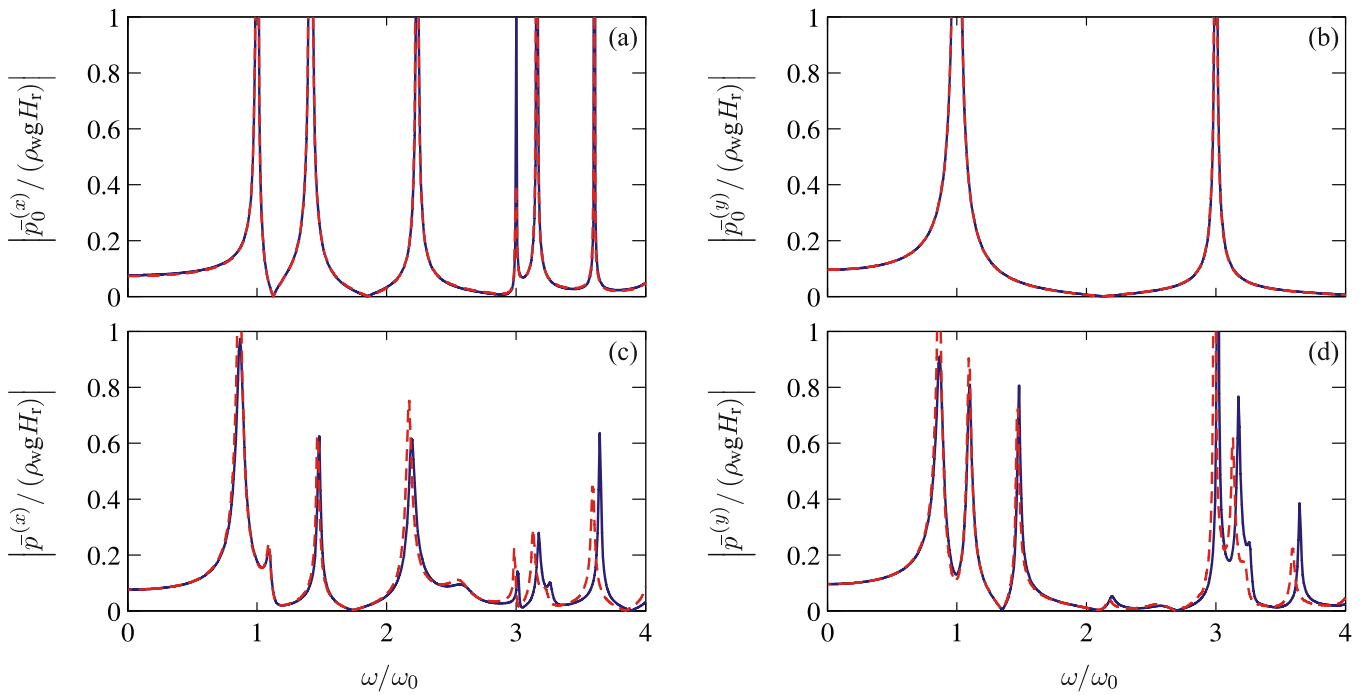


Figure 4. Absolute value of frequency response curves of normalized hydrodynamic pressures at the heel of the dam impounding a rectangular reservoir with $\alpha = 1.0$: (a) and (b) Rigid dam; (c) and (d) Flexible dam with 5% structural damping. – Analytical solution; -- Potential-based finite element solution.

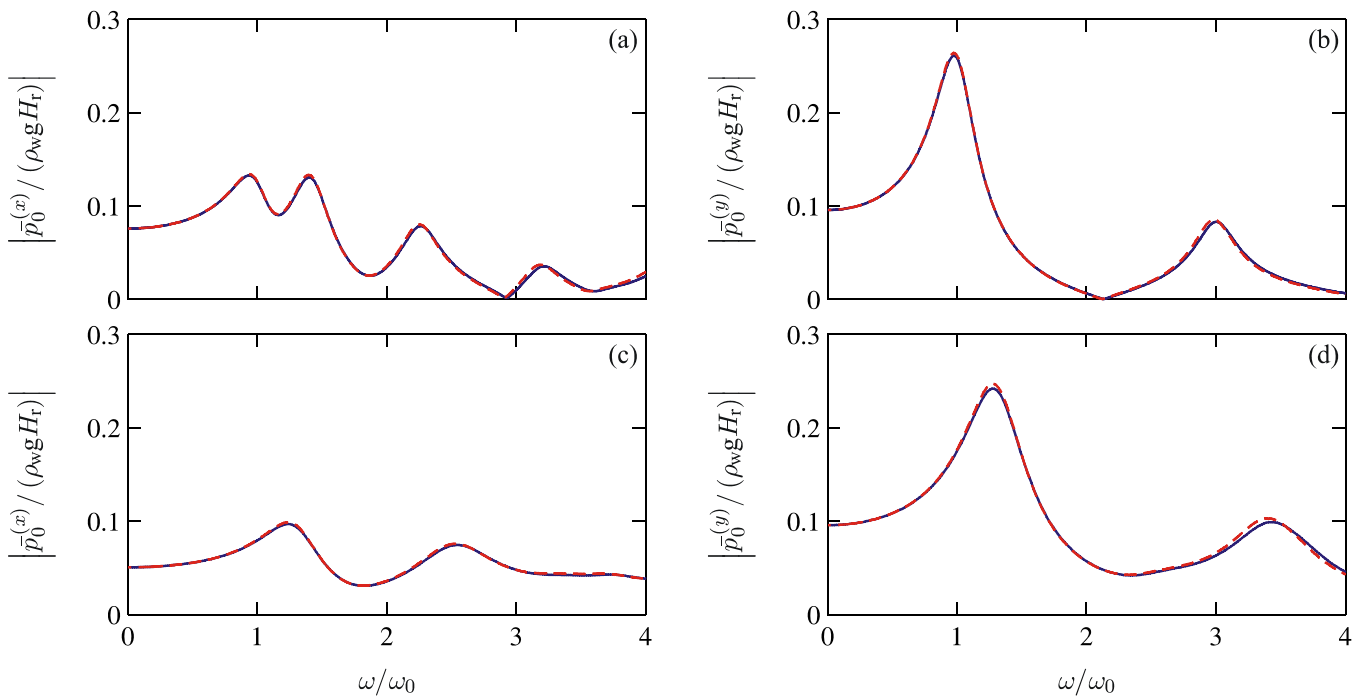


Figure 5. Absolute value of frequency response curves of normalized hydrodynamic pressures at the heel of the dam: (a) and (b) Rectangular reservoir with $\alpha = 0.6$; (c) and (d) Triangular reservoir with $\alpha = 0.6$. – Analytical solution; -- Potential-based finite element solution.

For the triangular reservoir (Figs. 5 (c) and (d)), finite element results are compared to a boundary element solution obtained using a program developed by the first author (Bouaanani and Paultre 2005). Figure 5 clearly shows that the potential-based finite element formulation combined with the viscous boundary condition give excellent results for wide frequency and wave absorption ranges. This potential-based formulation can also be efficiently used with other boundary conditions to account for energy dissipation at the reservoir far upstream or for dynamic interaction with an ice sheet covering the reservoir (Bouaanani and Chagnon 2006).

4. CONCLUSIONS

This paper presented simplified expressions and more advanced finite element techniques to assess the effect of fluid-structure interaction in seismically excited dam-reservoir systems. Several dam-reservoir systems with various shapes were used. The hydrodynamic frequency response curves obtained using the proposed methods were validated against analytical solutions when available and boundary element solutions otherwise. Excellent agreement is obtained over practical frequency and wave absorption ranges. The proposed techniques are shown to perform adequately for practical seismic analysis of dam-reservoir systems in frequency and time domains.

ACKNOWLEDGEMENTS

Financial support from the Natural Sciences and Engineering Research Council of Canada and the Quebec Fund for Research on Nature and Technology is gratefully acknowledged.

REFERENCES

- ADINA Theory and Modeling Guide. Report ARD 06-7. (2006). ADINA R & D, Inc.
- Bouaanani, N. Paultre, P., and Proulx, J. (2003). A closed-form formulation for earthquake-induced hydrodynamic pressure on gravity dams. *Journal of Sound and Vibration*, **33**, 573-582.
- Bouaanani, N. and Paultre, P. (2005). A new boundary condition for energy radiation in covered reservoirs using BEM. *Engineering analysis with boundary elements*, **29**: 9, 903-911.
- Bouaanani, N. and Chagnon, M-A. (2006). Seismic analysis of Ice-Dam-Reservoir systems. 1st International Structural Specialty Conference - Canadian Society of Civil Engineering, Calgary, May 23-26, Paper ST-100.
- Fenves, G. and Chopra, A.K. (1984). EAGD-84, a computer program for earthquake analysis of concrete gravity dams. Report No. UCB/EERC-84/11, University of California, Berkeley, California.
- Lysmer, J. and Kuhlemeyer, R.L. (1969). Finite dynamic model for infinite media. *Journal of the Engineering Mechanics Division, ASCE*, **95**, 859-877.
- Neilson, H.C., Everstine, G.C., and Wang, Y.F. (1981). Transient response of a submerged fluid-coupled double-walled shell structure to a pressure pulse. *Journal of the Acoustical Society of America*, **70**, 1176-1782.
- Everstine, G.C., Marcus, M.S., and Quezon, A.J. (1983). Finite element analysis of fluid-filled elastic piping systems. Eleventh Nastran User's Colloquium, May, 141-160.
- Landau, L.D. and Lifshitz, E.M. (1959). *Fluid mechanics*. Pergamon Press.
- Olson, L.G. and Bathe, K.J. (1985). Analysis of fluid-structure interactions: a direct symmetric coupled formulation based on the fluid velocity potential. *Computers and Structures*, **21**:1/2, 21-32.